Stability Issues in V/f Controlled Medium Voltage Induction Motor Drives Considering Magnetizing Inductance Variation

Simone Cosso, Krishneel Kumar, Mario Marchesoni, *Member, IEEE*, Massimiliano Passalacqua, *Member, IEEE*, and Luis Vaccaro, *Member, IEEE*

***Abstract*—In this article, a V/f control for high-power induction motor drives is analysed. In such uses, low dynamics in terms of speed-loop bandwidth is usually required. However, in some applications, where the load consists of a long shaft with certain mechanical components and with some resonant frequencies, instability and torque oscillations can cause significant damage. For these reasons, open-loop V/f control could be a winning solution, since it avoids resonances and oscillations caused by measurement feedbacks in the control. However, instability may arise also in open-loop V/f control. A stability analysis is here carried out analytically and a new method to overcome oscillations by varying dynamically the V/f ratio is proposed. The stability analysis and the effectiveness of the proposed method are verified with simulation results on a 2.8 kV-7.25 MW induction motor and with experimental tests on a small-scale 380 V-10 kW motor.**

***Index Terms*—Electrical drives, induction motor, stability, V/F control.**

I. Introduction

INDUCTION motors (IM) remain the best choice in several industrial applications. Closed-loop control methods, such as Field Oriented Control (FOC) [1], [2], [3], [4] and Direct Torque Control (DTC) [5], [6], [7], [8], [9], are mostly used to achieve high dynamic performance. However, in case of mechanical resonances, measurement feedbacks of closed-loop control could amplify the phenomenon. This aspect is particularly critical in Medium-Voltage (MV) drives; as a matter of facts, instability regions are usually wider in MV motors [10] and, moreover, the consequences are more serious. For these reasons, open-loop V/f control [11], [12], [13], [14], [15], [16], [17], [18], [19], [20], [21], [22], [23], which is usually used in low-cost drives for its simplicity, could be a valid alternative to closed-loop methods in some low-dynamics MV applications, with instabilities caused by mechanical resonance phenomena and where torque oscillations could lead to mechanical damages. However, even if open-loop control does not amplify the resonances coming from measurements, sometimes oscillations related to V/f technique may arise, especially at light load [10].

Oscillations with V/f technique is a topic highly studied in the technical literature. A small-signal linearization is carried out in [12], [13], [14], [15], [16] to evaluate V/f stability and pole locations in the f-V (frequency-voltage) plane [12], [13], [14], [15] or in the T-f (torque- frequency) plane [16]. Moreover, in [17] conditions for global asymptotic stability is given in terms of motor parameters, operating slips and synchronous frequency.

The typical solution to overcome these oscillations is to exploit active damping techniques based on current feedbacks. In [18], two Proportional-Integral control (PI) with current magnitude and angle as input are used to modify stator voltage amplitude and frequency. Similarly, a PI approach is carried out in [19], where the differential current acts on the stator voltage amplitude. In [20], Id is filtered with a Band Pass Filter (BPF); at low speed the BPF output modifies the stator voltage amplitude, whereas at high speed it modifies the stator voltage frequency. In [21], both Id and Iq are sent to a BPF, the difference between the filtered values is used to modify the stator voltage frequency. In [22], the same scheme of [21] is used; however a High Pass Filter (HPF) is used instead of a BPF. In [23] different strategies are tested: a HPF is applied to Iq and used to modify the direct-axis voltage (Vd), a HPF is applied to Id and used to modify the quadrature-axis voltage (Vq) and, finally, a HPF is applied to Id and used to modify the voltage frequency. The first solution was considered by the authors in [23] the most effective option.

These methods have all in common the fact that the stator current is used to modify the stator voltage amplitude and/or frequency. They are winning methods for low-power drives, where V/f control is chosen for its simplicity. However, when V/f is chosen in MV drives to overcome resonances coming from measurement feedbacks, active damping methods could fail, since they are not open-loop methods.

In this article, a novel open-loop method to overcome V/f oscillations is proposed. The model is based on the evaluation of the instability region on the f-V plane. Eigenvalues are evaluated for different voltage and frequency values. The iron saturation effect is taken into account since, as it will be shown in the article, it significantly influences the stability of the drive. The aim of the proposed algorithm is to modify appropriately the V/f ratio

Manuscript received 3 February 2023; revised 18 May 2023; accepted 20 June 2023. Date of publication 22 June 2023; date of current version 28 November 2023. Paper no. TEC-00105-2023. *(Corresponding author: Mario Marchesoni.)*

The authors are with the DITEN, University of Genova, 16145 Genova, Italy (e-mail: simone.cosso@edu.unige.it; krishneel.kumar@edu.unige.it; marchesoni@unige.it; massimiliano.passalacqua@unige.it; luis.vaccaro@unige.it).

Color versions of one or more figures in this article are available at https://doi.org/10.1109/TEC.2023.3288673.

Digital Object Identifier 10.1109/TEC.2023.3288673

for each synchronous frequency, in order to avoid the instability region. Since the evaluation is made a priori considering motor parameters, the proposed method is completely open-loop.

This method is particularly indicated for MV motors with low inertia, where instability and resonance phenomena are particularly critical.

A study on this idea was presented by the authors in [10]. In particular, it was proven how, modifying the flux reference with an Ad-Hoc Slope Ramping Algorithm (AHSRA), it was possible to avoid oscillations. However, at that stage, the linear model of the induction motor was considered. With this assumption, it seemed that it was necessary to reduce the motor flux to overcome the instability region. Of course, this was a strong limitation since just a limited torque was available during the speed ramp.

In this article, on the contrary, iron saturation effect on the stability region is taken into account. From this analysis, it is proven that the stability can be achieved also with a flux increase. In this way, the strong limitation of the method proposed in [10] is avoided since almost the rated torque is available for all the speed ramp.

The article is structured as follows: the stability analysis is shown in Section II. Simulation results with the proposed method applied to a 2.8 kV-7.25 MW motor are carried out in Section III, together with the simulation results on the motor used in the experimental test bench. Experimental results on a small-scale 380 V-10 kW motor are reported in Section IV and, finally, conclusions are carried out in Section V.

II. Small-Signal Model and Stability Analysis

The following analysis is done considering a squirrel-cage induction motor, which is nowadays the most common induction motor topology.

A. Small-Signal Model

The stability analysis of the non-linear model has to be performed through a linearization around a steady-state operating point. The small-signal model of the induction motor based on the standard dynamic equations in the synchronous d-q reference frame is expressed as in (1) [12]. Please note that the dead-time error voltages are also incorporated in the stator voltage equations, since the model represents an inverter fed induction motor.

$$\Delta \dot{x} = \mathbf{A}\Delta x + \mathbf{B}\Delta u \tag{1}$$

Where Δx is the state vector of the system, defined in (2):

$$\Delta x = [\Delta i_{qs} \Delta i_{ds} \Delta i'_{qr} \Delta i'_{dr} \Delta \omega_r]^T \tag{2}$$

and Δu is the input vector of the system, defined in (3):

$$\Delta u = [\Delta v_{qs} \Delta v_{ds} 00 \Delta T_l]^T \tag{3}$$

i_{qs}, i_{ds}, i'_{qr} and i'_{dr} represent the q-axis and d-axis components of the stator and rotor (referred to stator) currents, respectively. v_{qs} and v_{ds} are the stator q- and d-axis voltages. ω_r is the rotor electrical speed and T_l is the load torque.

TABLE I
Medium Power Motor Parameters

Quantity	Value
Rated output power Pn	7.25 MW
Number of poles P	2
Rated frequency Fn	38.6 Hz
Rated voltage Vn	2800 V
Rated current In	1712 A
Magnetizing current Is0	425 A
Stator resistance Rs	4 mΩ
Rotor resistance R'r	4.33 mΩ
Magnetizing inductance Lm	15.256 mH
Stator inductance Ls	15.4 mH
Rotor inductance L'r	15.7 mH
Moment of inertia J	130 Kgm^2
Rated torque Tn	30.82kNm

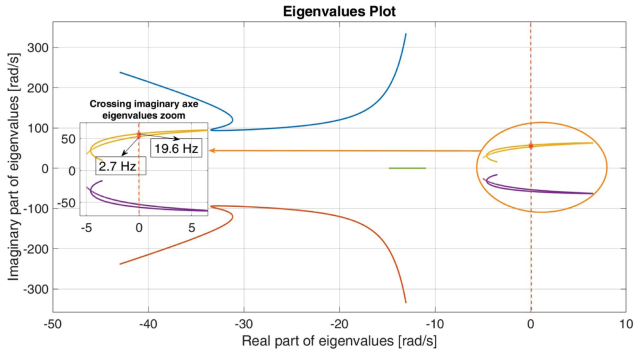

Fig. 1. Eigenvalues plot of the 7.25 MW motor varying the frequency in the range 0-38.6 Hz.

The resulting system matrix $\mathbf{A}$ is reported in (4), where the subscript "0" represent the steady-state operating point; please note that all the different submatrices are defined in [12].

$$\mathbf{A} = \begin{bmatrix} -\mathbf{L}^{-1}\mathbf{R} & -\mathbf{L}^{-1}\lambda_{10} \\ \left(\frac{3}{2J}\right)\left(\frac{P}{2}\right)^2 \lambda_{20}^{\mathrm{T}} & -\frac{B}{J} \end{bmatrix} \tag{4}$$

The presented small-signal model is used to perform a stability analysis of the system. The parameters of the 7.25 MW induction motor are reported in Table I [10].

The root locus varying frequency between 0 to 38.6 Hz (rated value) of the considered motor drive is obtained and shown in Fig. 1. The horizontal and vertical axes represent the real and imaginary parts of the roots. The complex conjugate pair, which is closer to the jω axis, has positive real parts, but only for frequencies ranging between 2.7 and 19.6 Hz as highlighted in Fig. 1.

If these unstable points are calculated varying the V/f ratio (please note that Fig. 1 refers to a V/f ratio equal to 1, i.e., rated flux) and plotted in the V-f plane, the region of instability can be obtained. In Fig. 2 the region of instability in the V-f plane is represented. Please note that the lowest unstable V/f ratio obtained is 0.06 p.u. in this case.

The effects of iron saturation are now considered in the discussion. Fig. 3 shows the classical saturation curve considered for the 7.25 MW motor in the current/voltage plane.

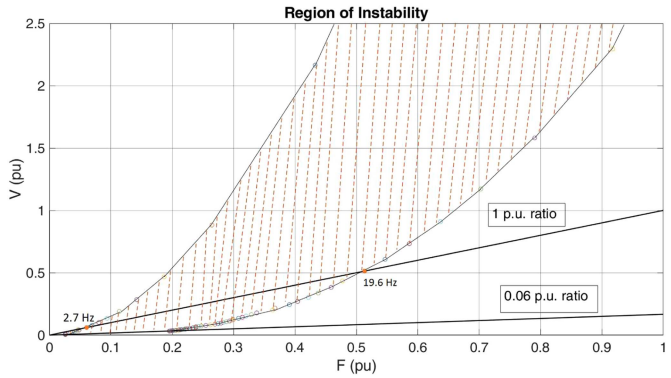

Fig. 2. Region of instability of the 7.25 MW motor in the V-f plane.

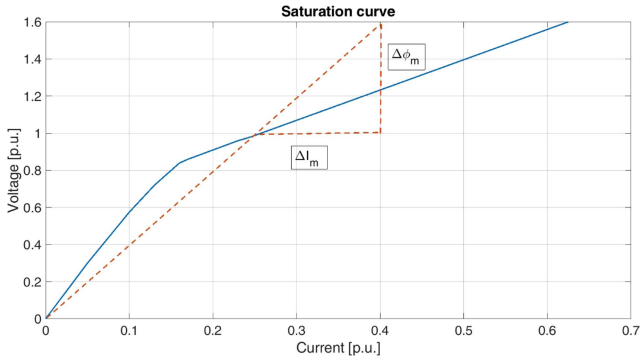

Fig. 3. Saturation curve of the 7.25 MW motor.

The magnetizing inductance resulting in the linearization of the saturation curve represents the rated value of the parameter, equal to 15.25 mH for the 7.25 MW induction motor (please note that for this motor the rated magnetizing current is 25% of the rated current). If one considers the inductance at a higher voltage value (i.e., at a higher flux value) the corresponding inductance L'_m becomes considerably lower. For example, the L'_m value for 1.6 p.u. flux is expressed in (5).

$$L'_{m,1.6p.u.} = \frac{\Delta\varphi'_m}{\Delta I'_m} \simeq \frac{2}{3} Lm \tag{5}$$

If for each flux value the corresponding value of L'_m is adopted, instead of the rated value of L_m, to calculate the region of instability of the machine, one can notice that the unstable operating points are significantly reduced, as shown in Fig. 5. Indeed, in Fig. 5 the instability region of the 7.25 MW induction motor with the consideration of the saturation effects of the iron is plotted.

In order to better highlight the region, a zoom between 0 p.u. and 0.5 p.u. frequency is reported in Fig. 5, where it is evident that the instability area is much smaller compared to Fig. 2. Indeed, the lowest unstable V/f ratio is 0.17 p.u. and the maximum unstable frequency at rated flux is 0.15 p.u. in Fig. 5. On the contrary, the lowest unstable V/f ratio is 0.06 p.u. and the maximum unstable frequency at rated flux is 0.52 p.u. in Fig. 2, where the saturation effects have not been included in the modelling.

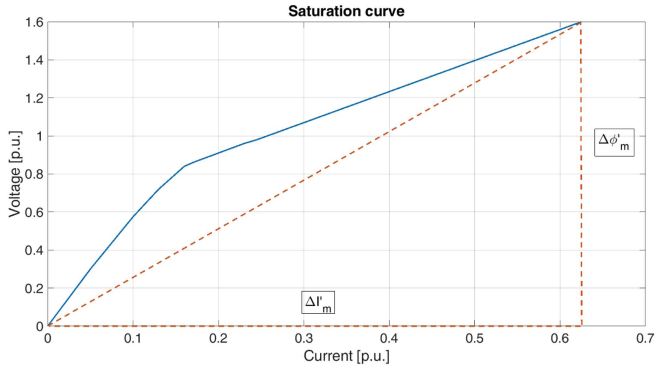

Fig. 4. Saturation curve of the 7.25 MW motor (incremental inductance).

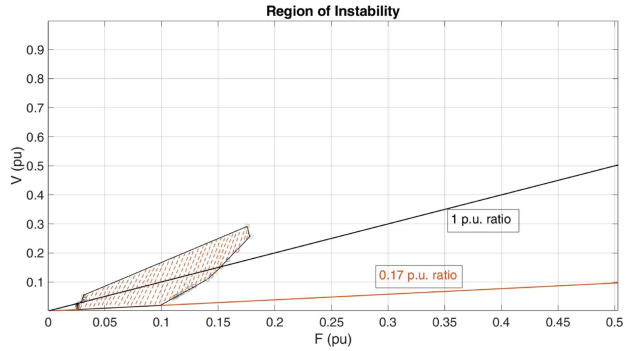

Fig. 5. Region of instability of the 7.25 MW motor in the V-f plane including the saturation curve in the modelling.

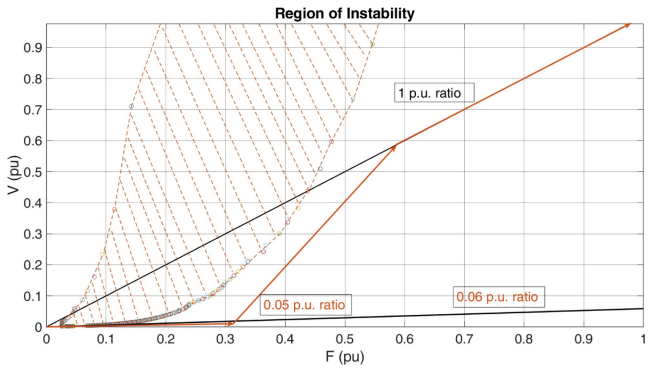

Fig. 6. Customized V/f ratio where saturation is not considered.

B. *Proposed Solution to Overcome Instability*

In this Section a novel method is proposed in order to avoid the operation of the induction machine inside the instability region, which does not require any feedback loop. In this technique, the V/f ratio is varied along with the different speeds of the drive. These different ratios are derived based on the plot of the instability region of the machine. From the instability region shown in Fig. 2, where the saturation effects have not been considered in the modelling, one can think that the only solution to avoid the instability is creating a customized slope ramp as reported in Fig. 6. In this condition the motor is under-fluxed until the instability zone is exceeded.

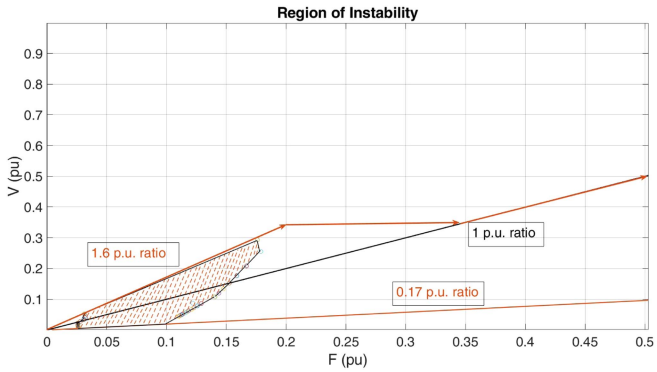

Fig. 7. Proposed solution to avoid the region of instability including saturation effects.

When the saturation is taken into account, the instability region gets smaller, as shown in the previous Section. Therefore, one can also avoid the oscillations by creating a customized slope ramp overfluxing the motor for low speeds, and gradually reducing the flux to the rated value when the instability region is exceeded. This proposed customized slope ramp is reported in Fig. 7.

Since the flux is greater than the rated value only for low speeds, the voltage is always lower than the rated value in the overfluxing region. One can notice that overfluxing the machine to avoid the instability region is not a solution one would consider adoptable, if the saturation is not taken into account in the stability analysis, as shown in Fig. 2.

In addition, please note that the method of Fig. 6 is not possible if a substantial starting torque is required.

Moreover, the instability region regards the low and medium speed region, approximately until 20-30% of the rated speed. Thus, even if the proposed solution is developed for the constant-torque rated-flux zone, there are no limitation for the motor to work in the flux-weakening region.

Finally, some considerations on current limitation should be done. Being the V/f an open-loop control, the speed ramp slope (i.e., the acceleration) should be carefully limited in order not to overload the motor. The maximum acceleration can be evaluated from the load inertia and the resistant torque. Once the maximum acceleration is known, one can set this limit in the drive with an opportune safety margin.

With the proposed method, there will be a higher magnetizing current during the motor speed ramp. The magnetizing current can be evaluated from the magnetizing curve shown in Fig. 4. Thus, one can calculate the maximum acceleration with the same approach used in a standard V/f control.

III. Simulation Results

In this Section, simulation results on two different induction motors are reported: the medium power motor considered in Section II for the stability analysis and a low power one. Please note that the aforementioned low power motor is the one considered in the experimental results in Section IV, therefore a comparison between simulations and experimental tests can be carried out.

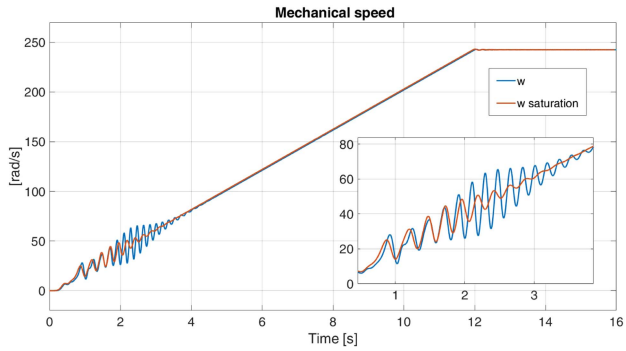

Fig. 8. Mechanical speed with 1 p.u. flux.

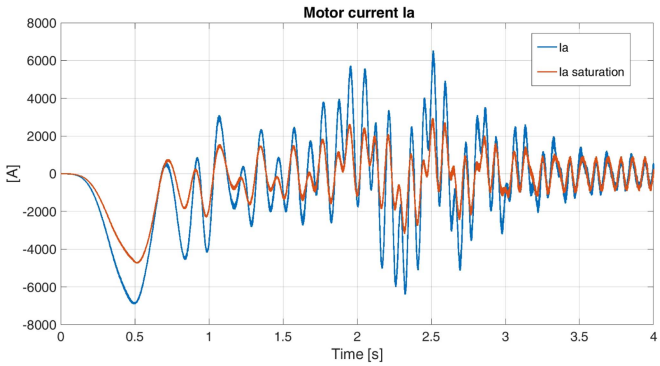

Fig. 9. Stator current Ia with 1 p.u. flux.

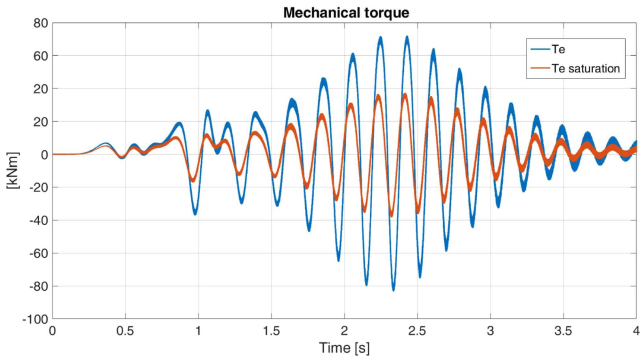

Fig. 10. Mechanical torque with 1 p.u. flux.

The classic open-loop V/f control logic has been implemented in MATLAB/Simulink environment, where a SIMSCAPE model of the induction machine has been employed, in order to include the saturation curve of the motor.

A 2-level PWM inverter model has been employed, where the switching frequency and the deadtime have been set to 5 kHz and 3 μs, respectively.

A. 7.25 MW Motor

In this Section, the medium voltage motor of Section II is considered, in order to validate what has been shown in the stability analysis.

The parameters of the 7.25 MW induction machine are reported in Table I, in Section II.

Figs. 8, 9, and 10 show the mechanical speed, the stator current, and the mechanical torque during an acceleration from

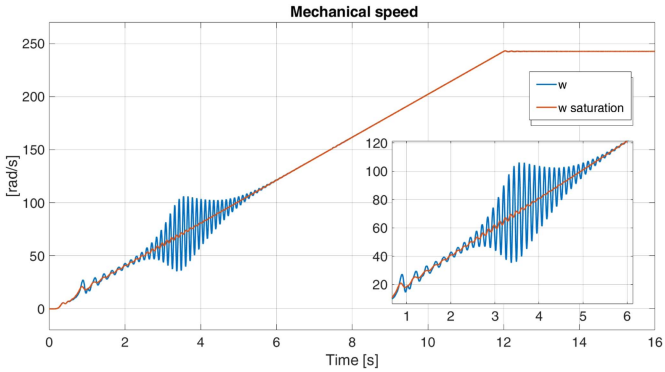

Fig. 11. Mechanical speed with 1.6 p.u. flux.

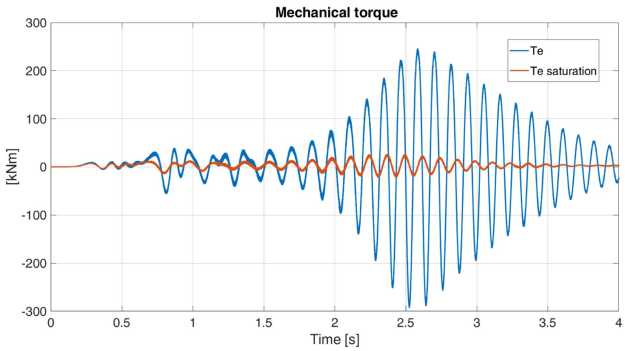

Fig. 13. Mechanical torque with 1.6 p.u. flux.

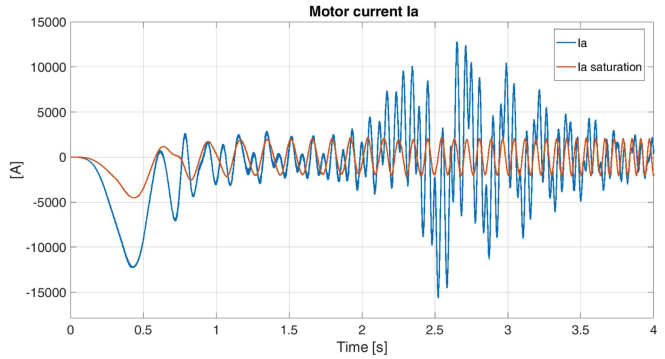

Fig. 12. Stator current Ia with 1.6 p.u. flux.

TABLE II
LOW POWER MOTOR PARAMETERS

Quantity	Value
Rated output Power Pn	9.75 kW
Number of poles P	4
Rated frequency Fn	50 Hz
Rated voltage Vn	380 V
Rated current In	15.6 A
Stator resistance Rs	0.66 Ω
Rotor resistance R'r	0.49 Ω
Magnetizing inductance Lm	0.09 H
Stator inductance Ls	0.1533 H
Rotor inductance L'r	0.1533 H
Rated torque Tn	62 Nm

0 rad/s to the rated speed of 242.2 rad/s with a constant flux of 1 p.u. The blue trace represents the simulation when the saturation curve is not considered in the model, while the red one represents the simulation with the inclusion of the saturation curve of the motor.

Please note that the complete simulation has been reported for the speed plots, whereas a zoom between 0 and 4 seconds is shown for the current and the torque plots, in order to highlight the oscillations due to the instability region.

Including the saturation curve in the model leads to obtain less oscillations. The same test with a flux of 1.6 p.u. is shown in Figs. 11, 12 and 13, where a consistent reduction of the oscillations can be appreciated if the saturation is taken into account.

By comparing the simulations, one can note that the saturation damps the oscillations, even though they are not completely suppressed, as shown in the stability analysis in Section II. It can also be noticed from the current and torque plots that the oscillations are gradually reduced when the flux is increased. Indeed the torque oscillation amplitudes in Fig. 13 are about 15 kNm (considering saturation, red trace), whereas they are about 50 kNm in Fig. 10. Please note that if the saturation is not taken into account (blue trace), torque oscillations at 1.6 p.u. flux are considerably higher than the torque oscillations at 1 p.u. flux. Please note that since these are simulation results, it was possible to overflux the motor also at rated speed. In addition, it should be pointed out that the average mechanical torque value is the one related to the acceleration reference, which is not zero, although this is difficult to acknowledge due to oscillations amplitude.

B. 9.75 kW Motor

Table II contains the parameters of the 9.75 kW induction motor, while the measured saturation curve of the motor is reported in Fig. 14.

The region of instability of the 9.75 kW motor is reported in Fig. 15. Please note that saturation effects have been taken into account in the stability analysis, analogously to what has been shown for the 7.25 MW machine in Fig. 5. It can be noted from Fig. 15 that the lowest unstable V/f ratio is 0.53 p.u. and the maximum unstable frequency at rated flux is 0.275 p.u.

Simulations have been executed for the 9.75 kW motor and the results are reported in the following figures. In this case only mechanical speed and stator current are reported.

Figs. 16 and 17 show the mechanical speed and the stator current during an acceleration from 0 rad/s to the rated speed of 157 rad/s with a constant flux of 0.7 p.u., respectively.

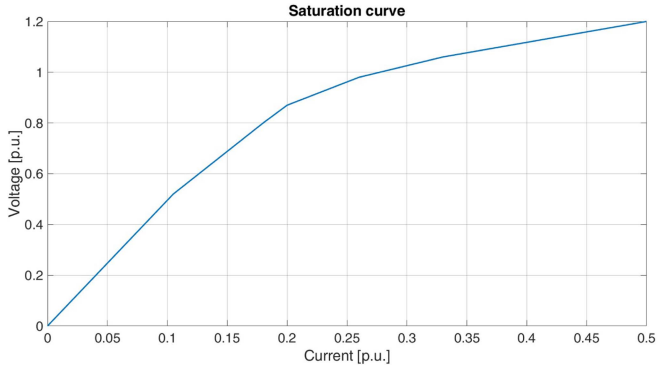

Fig. 14. Saturation curve of the 9.75 kW motor.

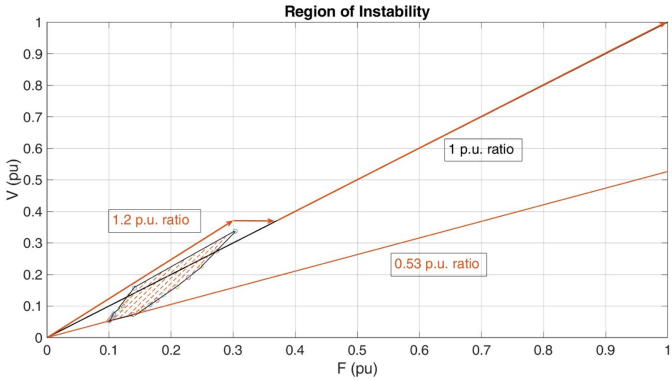

Fig. 15. Region of instability of the 9.75 kW motor.

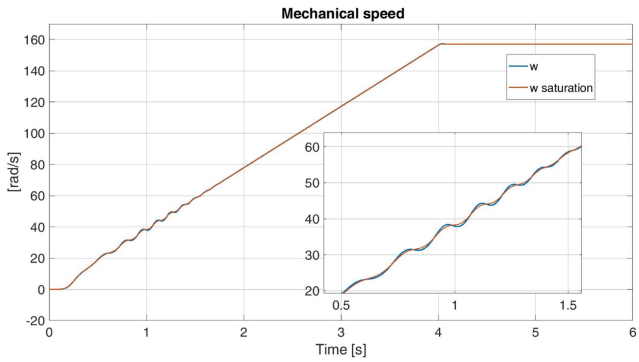

Fig. 16. Mechanical speed with 0.7 p.u. flux.

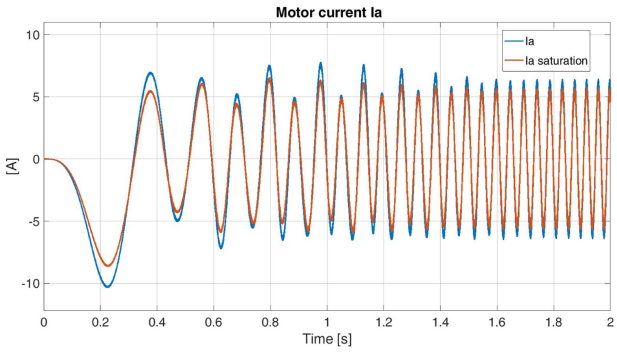

Fig. 17. Stator current Ia with 0.7 p.u. flux.

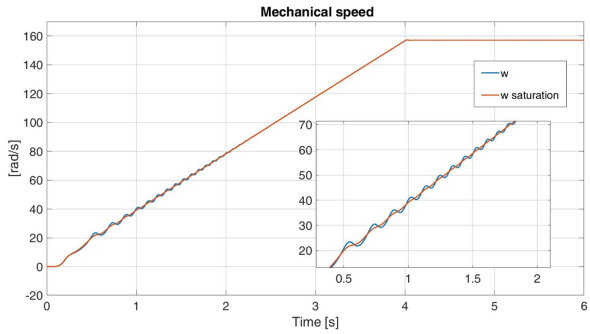

Fig. 18. Mechanical speed with 1 p.u. flux.

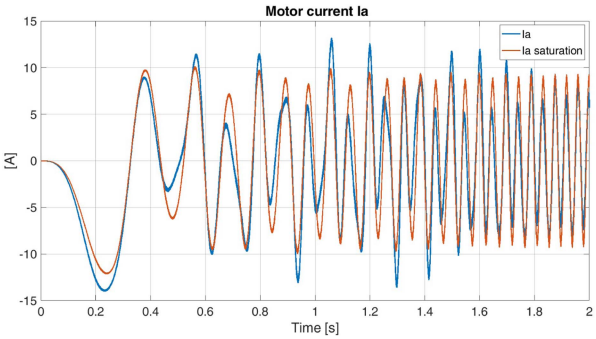

Fig. 19. Stator current Ia with 1 p.u. flux.

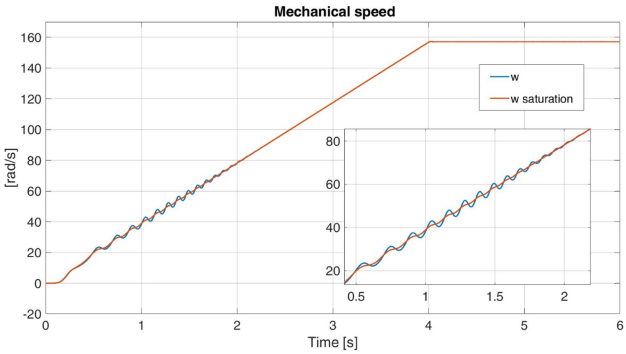

Fig. 20. Mechanical speed with 1.2 p.u. flux.

In this case, including the saturation in the model does not lead to relevant discrepancies in the graphs, even if a reduction of the oscillations can be highlighted. As reported for the 7.25 MW motor, the results with and without the saturation curve (red and blue, respectively) are shown together. The same test has been repeated with 1 p.u. flux (rated flux) and with 1.2 p.u. flux, and the results have been reported in Figs. 18, 19, 20, and 21, respectively.

By comparing the simulations, analogously to what reported for the medium power motor, one can note that the oscillations are damped by the saturation effects, as shown in the stability analysis in Section II. Please note that since these are simulation results, it was possible to overflux the motor also at rated speed.

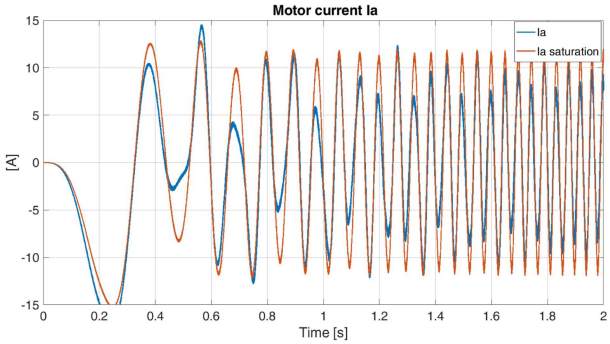

Fig. 21. Stator current Ia with 1.2 p.u. flux.

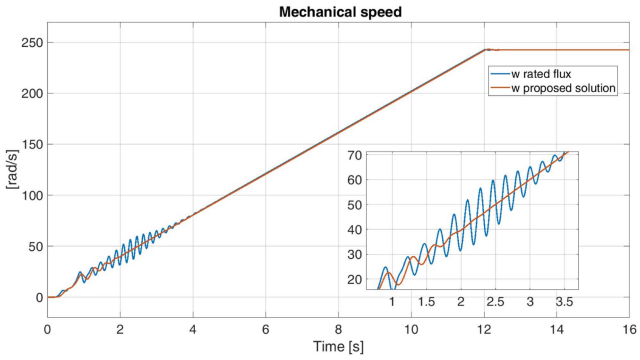

Fig. 22. Mechanical speed with proposed method (red), and with rated flux (blue) (7.25 MW).

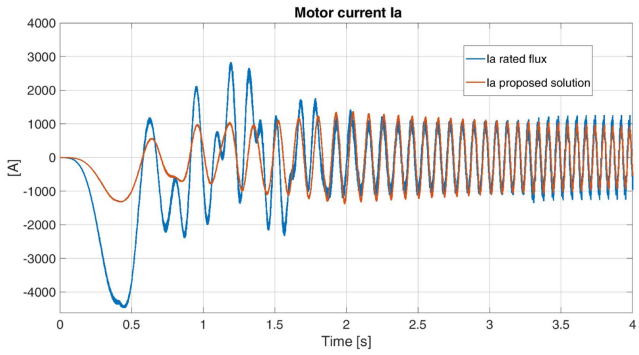

Fig. 23. Stator current Ia with proposed method (red), and with rated flux (blue) (7.25 MW).

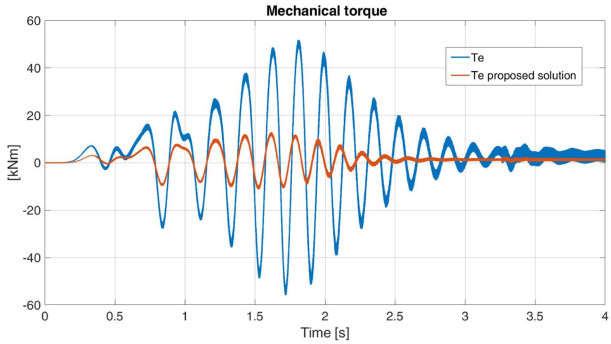

Fig. 24. Mechanical torque with proposed method (red), and with rated flux (blue) (7.25 MW).

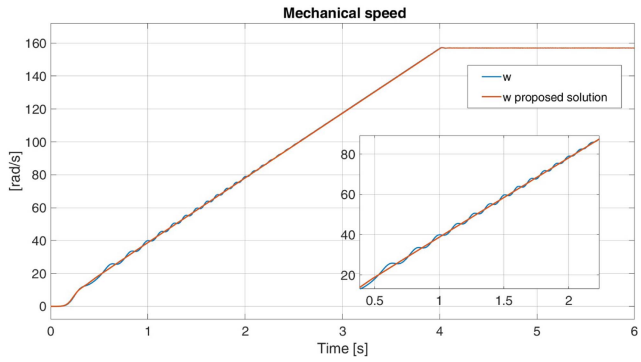

Fig. 25. Mechanical speed with the proposed method (red), and with rated flux (blue) (9.75 kW).

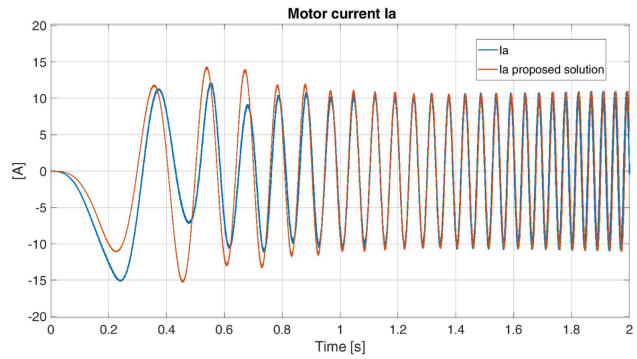

Fig. 26. Stator current Ia with proposed method (red), and with rated flux (blue) (9.75 kW).

C. Proposed Solution Results

In this Section, some results obtained with the proposed method, introduced in Section II, are reported for the 7.25 MW and the 9.75 kW motors, respectively. As regard the medium voltage machine, it has been started with a flux equal to1.6 p.u. for the first 2.8 s, then it was linearly decreased at 1.4 p.u. at 3.6 s, and finally returned at rated value of 1 p.u. at 4 s, in accordance to what it is shown in Fig. 7. Fig. 22 shows the mechanical speed during the acceleration until the rated speed of 242 rad/s, while Figs. 23 and 24 show the zoom between 0 and 4 seconds of the stator current and the mechanical torque, respectively. Please note that the blue traces represent current and torque behaviours using the rated flux slope ramp, whereas the red traces represent the behaviours of the same quantities using the proposed solution.

It can be noticed that the proposed method accurately mitigates the oscillations, since the instability region is avoided. Moreover, please note that the torque oscillations in the red trace of Fig. 24 are less than 10 kNm, against the 60 kNm of the rated flux simulation, therefore an effective reduction of the oscillations is achieved.

Fig. 27. Test bench.

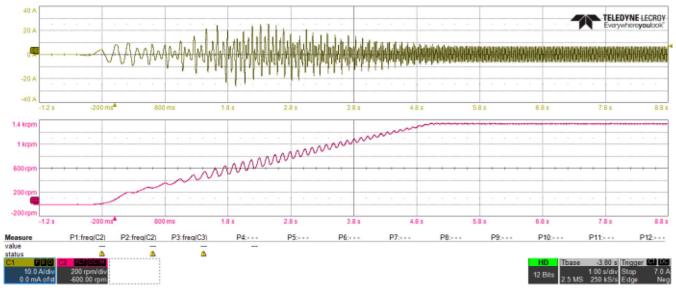

Fig. 28. Mechanical speed (red), and stator current (green) with 0.7 p.u. flux.

Figs. 25 and 26 show the comparison of the results obtained using the proposed technique and the rated flux ramp, respectively, with the 9.75 kW motor, during the acceleration until the rated speed of 157 rad/s. In this case, for the proposed solution, the flux is kept at 1.2 p.u for 1 s, then it is linearly decreased at the rated value at 2 s. The mechanical speed is reported in Fig. 25, while the stator current of phase a is shown in Fig. 26. Please note that for this low power machine the differences are less significant, since the amplitude of the oscillations due to the instability region is smaller compared to the medium power machine. However, the proposed method allows speed oscillations reduction also in this case.

IV. Experimental Results

Experimental tests have been carried out in order to validate the theoretical analysis and the method proposed in this article. The V/f control logic has been implemented in DSpace Microlab Box control platform and the test bench is shown in Fig. 27.

The DSpace system outputs have been sent to an inverter with DC link voltage of 550 V connected to the induction machine. Both the sampling frequency and the PWM switching frequency have been set to 5 kHz, whereas the dead time was set to 3 μs, according to what has been done in the theoretical stability analysis and in simulations.

Figs. 28 and 29 show the mechanical speed (red) and the stator current (green) during an acceleration until the rated speed of 157.6 rad/s with a constant 0.7 p.u. flux, while the results related to 1 p.u. flux are reported in Figs. 30 and 31, respectively.

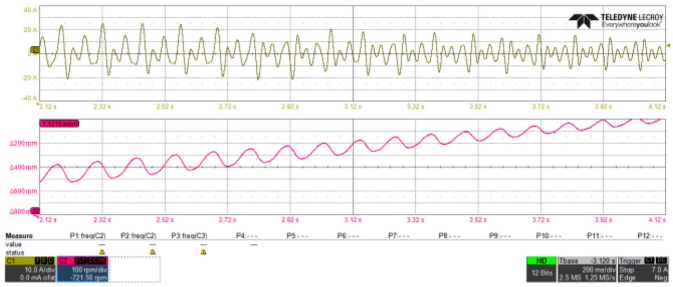

Fig. 29. Zoom of mechanical speed (red), and stator current Ia (green) with 0.7 p.u. flux.

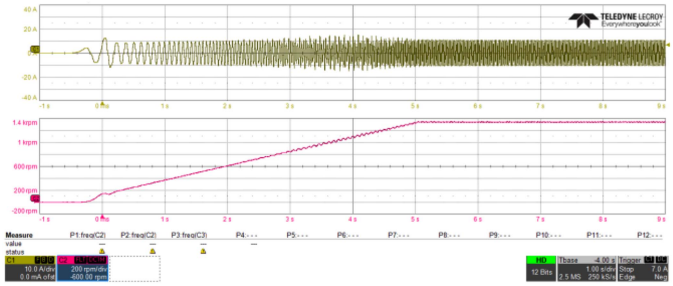

Fig. 30. Mechanical speed (red), and stator current Ia (green) with 1 p.u. flux.

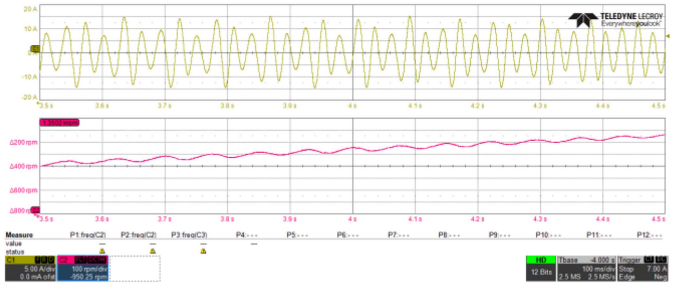

Fig. 31. Zoom of mechanical speed (red), and stator current Ia (green) with 1 p.u. flux.

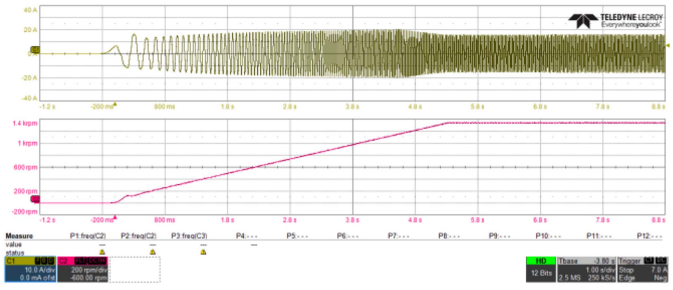

Fig. 32. Mechanical speed (red), and phase a stator current Ia (green) with the proposed overfluxed ramp.

Fig. 32 shows the results using the customized slope ramp proposed in this article. In this case, the flux is kept at 1.2 p.u for the first 4 s, then it linearly decreases, in order not to saturate the voltage, until the rated value of 1 p.u. is reached at 5 s.

By comparing the results during the three different tests, one can note that using the customized slope ramp can lead to a significant reduction of the oscillations, since the region of instability is avoided. Moreover, a great correspondence between the simulation results and the experimental results can be observed. Finally, one has to note that the oscillation at rated flux with the 9.75 kW motor are not really critical. Actually, the proposed method is useful especially for MV motors. However, 9.75 kW motor was considered to validate the proposed analysis with small-scale experimental tests.

V. Conclusion

In this article, a new open-loop method to avoid oscillations in V/f control of induction motor is considered. Firstly, a stability analysis is performed, considering the instability region on the frequency-voltage plane; iron saturation is taken into account since it significantly influences the stability. Then, the proposed method is shown, which is based on V/f ratio variation, in order to avoid the instability area. This method is particularly indicated for MV motors, where the instability region is large and the oscillation effects are more critical. The proposed solution is verified with simulations on a 7.25 MW induction motor, where torque oscillations are reduced by about 80% compared to the rated V/f ratio case. The proposed analysis is then validated with small-scale experimental tests on a 9.75 kW induction motor, comparing simulation and experimental results. A great correspondence between simulations and experiments can be observed and the analysis is therefore validated. This study can greatly improve the classic open loop V/f control and make it suitable in some high power applications. The proposed method may be sometimes preferable to certain closed-loop control systems, in theory more performing but sometimes more critical, especially in cases of mechanical resonances, where the needed measurement feedbacks could amplify instability phenomena.

References

[1] M. S. N. Said and M. E. H. Benbouzid, "Induction motors direct field oriented control with robust on-line tuning of rotor resistance," *IEEE Trans. Energy Convers.*, vol. 14, no. 4, pp. 1038–1042, Dec. 1999.

[2] J. Chen, J. Huang, and Y. Sun, "Resistances and speed estimation in sensorless induction motor drives using a model with known regressors," *IEEE Trans. Ind. Electron.*, vol. 66, no. 4, pp. 2659–2667, Apr. 2019.

[3] M. S. Zaky, M. K. Metwaly, H. Z. Azazi, and S. A. Deraz, "A new adaptive SMO for speed estimation of sensorless induction motor drives at zero and very low frequencies," *IEEE Trans. Ind. Electron.*, vol. 65, no. 9, pp. 6901–6911, Sep. 2018.

[4] M. Tousizadeh, H. S. Che, J. Selvaraj, N. A. Rahim, and B. Ooi, "Fault-tolerant field-oriented control of three-phase induction motor based on unified feedforward method," *IEEE Trans. Power Electron.*, vol. 34, no. 8, pp. 7172–7183, Aug. 2019.

[5] F. Khoucha, M. S. Lagoun, A. Kheloui, and M. E. H. Benbouzid, "A comparison of symmetrical and asymmetrical three-phase h-bridge multilevel inverter for DTC induction motor drives," *IEEE Trans. Energy Convers.*, vol. 26, no. 1, pp. 64–72, Mar. 2011.

[6] Y. S. Lai and J. H. Chen, "A new approach to direct torque control of induction motor drives for constant inverter switching frequency and torque ripple reduction," *IEEE Trans. Energy Convers.*, vol. 16, no. 3, pp. 220–227, Sep. 2001.

[7] X. Wu, W. Huang, X. Lin, W. Jiang, Y. Zhao, and S. Zhu, "Direct torque control for induction motors based on minimum voltage vector error," *IEEE Trans. Ind. Electron.*, vol. 68, no. 5, pp. 3794–3804, May 2021.

[8] I. M. Alsofyani and K. B. Lee, "Enhanced performance of constant frequency torque controller–based direct torque control of induction machines with increased torque-loop bandwidth," *IEEE Trans. Ind. Electron.*, vol. 67, no. 12, pp. 10168–10179, Dec. 2020.

[9] I. M. Alsofyani, Y. Bak, and K. Lee, "Fast torque control and minimized sector-flux droop for constant frequency torque controller based DTC of induction machines," *IEEE Trans. Power Electron.*, vol. 34, no. 12, pp. 12141–12153, Dec. 2019.

[10] L. Carbone, S. Cosso, K. Kumar, M. Marchesoni, M. Passalacqua, and L. Vaccaro, "Stability analysis of open-loop V/Hz controlled asynchronous machines and two novel mitigation strategies for oscillations suppression," *Energies*, vol. 15, no. 4, 2022, Art. no. 1404.

[11] K. Lee and Y. Han, "Reactive-power-based robust MTPA control for v/f scalar-controlled induction motor drives," *IEEE Trans. Ind. Electron.*, vol. 69, no. 1, pp. 169–178, Jan. 2022.

[12] A. Guha and G. Narayanan, "Small-signal stability analysis of an open-loop induction motor drive including the effect of inverter deadtime," *IEEE Trans. Ind. Appl.*, vol. 52, no. 1, pp. 242–253, Jan./Feb. 2016.

[13] T. A. Lipo and P. C. Krause, "Stability analysis of a rectifier-inverter induction motor drive," *IEEE Trans. Power App. Syst.*, vol. PAS-88, no. 1, pp. 55–66, Jan. 1969.

[14] R. Ueda, T. Sonoda, K. Koga, and M. Ichikawa, "Stability analysis in induction motor driven by V/f controlled general-purpose inverter," *IEEE Trans. Ind. Appl.*, vol. 28, no. 2, pp. 472–481, Mar./Apr. 1992.

[15] R. Ueda, T. Sonoda, and S. Takata, "Experimental results and their simplified analysis on instability problems in PWM inverter induction motor drives," *IEEE Trans. Ind. Appl.*, vol. 25, no. 1, pp. 86–95, Jan./Feb. 1989.

[16] M. Hinkkanen, L. Tiitinen, E. Mölsä, and L. Harnefors, "On the stability of volts-per-hertz control for induction motors," *IEEE J. Emerg. Sel. Topics Power Electron.*, vol. 10, no. 2, pp. 1609–1618, Apr. 2022.

[17] A. Oteafy and J. Chiasson, "A study of the Lyapunov stability of an open-loop induction machine," *IEEE Trans. Control Syst. Technol.*, vol. 18, no. 6, pp. 1469–1476, Nov. 2010.

[18] Y. Q. Xiang, "Instability compensation of V/Hz PWM inverter-fed induction motor drives," in *Proc. IEEE Conf. Rec. Ind. Appl. Conf. 32nd IAS Annu. Meeting*, 1997, pp. 613–620.

[19] Z. Ma, F. Lin, and T. Q. Zheng, "A new stabilizing control method for suppressing oscillations of V/Hz controlled PWM inverter-fed induction motors drives," in *Proc. IEEE 37th Power Electron. Specialists Conf.*, 2006, pp. 1–4.

[20] J.-H. Jung, G.-Y. Jeong, and B.-H. Kwon, "Stability improvement of V/f-controlled induction motor drive systems by a dynamic current compensator," *IEEE Trans. Ind. Electron.*, vol. 51, no. 4, pp. 930–933, Aug. 2004.

[21] K. Suzuki, S. Saito, T. Kudor, A. Tanaka, and Y. Andoh, "Stability improvement of V/F controlled large capacity voltage-source inverter fed induction motor," in *Proc. IEEE Conf. Rec. Ind. Appl. Conf. 41st IAS Annu. Meeting*, 2006, pp. 90–95.

[22] Z. Qian, W. Yao, and K. Lee, "Stability analysis and improvement of V/Hz controlled adjustable speed drives equipped with small DC-link thin film capacitors," in *Proc. IEEE Appl. Power Electron. Conf. Expo.*, 2018, pp. 861–866.

[23] S. Zhang, J. Kang, and J. Yuan, "Analysis and suppression of oscillation in V/F controlled induction motor drive systems," *IEEE Trans. Transp. Electrific.*, vol. 8, no. 2, pp. 1566–1574, Jun. 2022.

Simone Cosso was born in Genoa, Italy in 1994. He received the B.S. and M.S. degrees in electrical engineering in 2016 and 2019, respectively, from the University of Genoa, Genoa, Italy, where he is currently working toward the Ph.D. degree with the Department of Electrical, Electronic and Telecommunication Engineering and Naval Architecture. His research interests include power converters and control for electrical drives.

Krishneel Kumar was born in Ba, Fiji, in 1994. He received the B.S. and M.S. degrees from the University of South Pacific, Suva, Fiji, in 2016 and 2018, respectively. He is currently working toward the Ph.D. degree with the Department of Electrical, Electronic and Telecommunication Engineering and Naval Architecture (DITEN), University of Genoa, Genoa, Italy. His research interests include power converters and control for electrical drives.

Mario Marchesoni (Member, IEEE) received the M.S. (Hons.) degree in electrical engineering and the Ph.D. degree in electrical engineering in power electronics from the University of Genova, Genova, Italy, in 1986 and 1990, respectively. Following his graduation, he began his research activity with the Department of Electrical Engineering, University of Genova, where he was an Assistant Professor from 1992 to 1995. From 1995 to 2000, he joined the Department of Electric and Electronic Engineering, University of Cagliari, Cagliari, Italy, where he was a Full Professor of power industrial electronics. Since 2000, he has been with the University of Genova, where he is currently a Full Professor of electrical drives control. His research interests include power electronics, with particular reference to high power systems for grid and motor applications, electrical systems for transportation, electrical drives, electrical machines, and automatic control. He was the General Chairman of the EPE'19 ECCE Europe Conference. His technical and scientific activity, certified by about 220 papers mainly presented at international conferences and published on international journals, has been carried out within research contracts and co-operations with national and international companies.

Massimiliano Passalacqua (Member, IEEE) was born in Genoa, Italy, in 1993. He received the B.S. (Hons.), M.S. (Hons.), and Ph.D. degrees in electrical engineering from the University of Genoa, Genoa, Italy, in 2015, 2017, and 2021, respectively. He is currently a Research Fellow with the Department of Electrical, Electronic and Telecommunication Engineering and Naval Architecture, University of Genoa. His research interests include power electronics, control for electrical drives, and hybrid electric vehicles.

Luis Vaccaro (Member, IEEE) was born in Chile. He received the B.Sc. degree in theoretical physics from the University of Concepcion, Concepcion, Chile, in 1991, and the M.Sc. degree in nuclear physics and the Ph.D. degree in electrical engineering from the University of Genoa, Genova, Italy, in 1995 and 2009, respectively. In 2004, he joined the team of power electronics with the University of Genoa. His primary research interests include multilevel converters, predictive control, hybrid electric vehicles, and renewable energies.